Optimized Ultrasonic Irradiation Finds Out Ultra-stable Aβ_{1-40} Oligomer

Kichitaro Nakajima,[†] Masatomo So,[‡] Kazuma Takahashi,[¶] Yoh-ichi Tagawa,[¶] Masahiko Hirao,[†] Yuji Goto,[‡] and Hirotsugu Ogi[*,†]

[†]*Graduate School of Engineering Science, Osaka University, Toyonaka, Osaka 560-8531, Japan*

[‡]*Institute for Protein Research, Osaka University, Suita, Osaka 565-0871, Japan*

[¶]*School of Life Science and Technology, Tokyo Institute of Technology, 4259 B51, Nagatsuta-cho, Midori-ku, Yokohama, Kanagawa 226-8501, Japan*

E-mail: ogi@me.es.osaka-u.ac.jp

Phone: +81-6-6850-6187. Fax: +81-6-6850-6187

Abstract

Oligomer species of amyloid β (Aβ) peptides are intensively investigated because of their relevance to Alzheimer's disease (AD), and a stable oligomer will be a cause for AD. In this paper, we investigate structural stability of two representative Aβ_{1-40} oligomers, which are with and without the β-sheet structure, denoted as β and non-β oligomers, respectively, using the optimized ultrasonic irradiation (OUI). Recent studies reveal that OUI significantly accelerates the fibril formation of Aβ_{1-40} monomers; it will be capable of transforming any unstable oligomers into the fibrils (the dead-end products) in a short time. First, we find that the β oligomers can be produced under the high-speed stirring agitation; their β-sheet structures are evaluated by the CD spectrum measurement, immunoassay using the fibril-specific OC antibody, and the seeding

experiment, showing the identical characteristics to those formed in previous reports. Second, we form the non-β oligomers under a high-concentration NaCl solution, and confirm that they include no β-sheet structure, and they are recognized by the oligomer-specific A11 antibody. Furthermore, we confirm the neurotoxicity of the two types of oligomers using neural tissue derived from mouse embryonic stem cell. We apply the OUI agitation to the β and non-β oligomers. The non-β oligomers are transformed into the fibrils, indicating that they are intermediate species on the fibrillation pathway. However, the β oligomers are surprisingly unaffected by OUI, indicating their high thermodynamic stability. We conclude that the β oligomers should be the independent dead-end products of another pathway, different from the fibrillation pathway.

INTRODUCTION

Aggregation reaction of amyloid β (Aβ) peptide has been investigated as a key factor on the pathology of Alzheimer's disease (AD). It is expected that Aβ aggregates show various functions and morphologies, depending on their chemical structures.[1,2] Characteristics of oligomers and amyloid fibrils have been central issues in AD related studies, because they are possible candidates of pathogenic species.[3] Although amyloid fibrils are recognized as toxic aggregates in most amyloidoses,[4,5] many studies indicate cytotoxicity of oligomer species of Aβ rather than the amyloid fibrils.[6–8] These backgrounds guide many researchers in studies of structure and function of Aβ oligomer species.[7,9]

Recently, two kinds of oligomers are intensively focused; oligomers with and without β-sheet structures. (We here denote them as β and non-β oligomers, respectively.) Kayed and coworkers confirmed deposition of the non-β oligomers on the entorhinal cortex in brain tissue of AD patient, suggesting that they are deeply related to the pathology of AD.[10] They also found that the non-β oligomers of Aβ peptides transformed into fibrils and indicated that the non-β oligomers were intermediates on the pathway for fibrils.[10,11]

The β oligomers are expected to possess β-sheet structures, because their circular-

dichroism (CD) spectra[12] and Fourier transform-infrared (FTIR) spectra[13] are similar to those of the Aβ fibrils. They are recognized by the fibril-specific antibody (OC antibody). They are also positive in the thioflavin-T (ThT) assay, although its level is lower than that for fibrils.[13] However, they cannot work as seeds for fibril formation.[13] These observations indicate that the β-sheet structure of the β oligomer is distorted compared with that in fibrils. Stroud and coworkers propose that the structure is composed of a twisted protofilament.[14]

In previous studies, the β oligomers of Aβ_{1-40} were prepared with a long-time ($\sim$48 h) aggregation reaction.[13] However, we here find that they can be briefly formed by a high-speed-stirring (HSS) agitation ($\sim$800 rpm): The ThT-positive aggregates are formed by the HSS agitation in a few hours, and their CD spectra indicate existence of β-sheet structure, but their transmission-electron-microscopy (TEM) images show spherical (non-fibril) particles. They fail to be seeds for the amyloid fibril. Furthermore, they are specifically recognized by the OC antibody. They also show neurotoxicity. These characteristics are identical to those of the β oligomers previously reported.[11–14]

There is then an open question; "Are the β oligomers intermediates for the amyloid-fibril dead end like the non-β oligomers?" This is particularly interesting in the thermodynamic point of view in aggregation reaction. Oligomer species of Aβ are often recognized as on-pathway intermediates for fibrils.[15,16] The β oligomers were also regarded as the intermediates.[11,14] For example, it was reported that the ThT level significantly grew when the β oligomers in ammonium hydroxide solution were dissolved in phosphate buffer saline(PBS) solution, suggesting that the β oligomer would not be independent dead-end aggregates.[14] However, this observation fails to be a robust proof of the intermediates, because the β oligomers could be dissolved into monomers and then form the fibrils, following the different pathways. Actually, Adachi and coworkers indicate that an oligomer is a dead-end product on the different pathway from that for fibril;[17] formations of fibrils and oligomers occur competitively, and their exchange is also made possible by the backward reaction process from each other based on Ostwald's ripening rule.[18] Miti and coworkers also regard oligomer

precipitate as an independent dead-end product in hen-egg-white-lysozyme aggregation.[19] In the previous studies, the states of aggregates were evaluated by changing protein concentration, solution temperature, solution pH, and additives affecting to the aggregation reaction such as NaCl and surfactants.[17,19] Because these parameters apparently vary the energy barriers for various aggregation species, both intermediate and dead-end oligomers (if any) will eventually reach to stable fibril state, through the reversed process from the dead-end oligomer to monomers. Therefore, distinction between on- and off-pathway oligomers is not straightforward with conventional chemical and thermal agitations.

In this study, we focus on ultrasonic irradiation as an effective agitation method for evaluating stability of protein aggregates. Recently, it is revealed that ultrasonic irradiation shortly induces protein fibrils,[20–22] and we find that this fibril formation can be drastically accelerated by optimizing the ultrasonic frequency and pressure.[23] (There is a direct pathway from monomers to fibrils caused by the cavitation effect[23,24] as will be explained later.) The optimized ultrasonic irradiation (OUI) is a powerful agitation tool for transforming the monomer state into the fibril dead end. On the other hand, it is generally recognized that ultrasonication is capable of decomposing aggregates composed of weakly interacting peptides (so called decomposition reaction under ultrasonic irradiation). Therefore, OUI will decompose any unstable intermediates into monomers, and then, create the fibrils because of the cavitation effect. If a stable dead-end product is produced, OUI will fail to affect it. These two effects (fibrillation by cavitation and decomposition of unstable aggregates) allow us to evaluate existence of a stable dead-end product. This is a principal issue in this study.

First, we investigate the relationship between the stirring speed and the reaction velocity constant for formation of β oligomers using the ThT fluorescence assay. The result indicates necessity of the static shear-stress field for formation of the β oligomers. Second, the immunoassay using OC and A11 antibodies are performed with wireless-electrodeless quartz-crystal-microbalance (WE-QCM) system which we previously developed.[25,26] Our β oligomers positively react to the OC antibody, but not to the A11 antibody, being identical to

the β oligomers previously reported.[11] Third, the seeding experiments for various aggregates are performed. The result shows that β oligomers fail to work as seeds for fibrils, indicating that they possess distorted β-sheet structures. Fourth, the neurotoxicity of the β and non-β oligomers is evaluated using the nerve system formed by mouse embryonic stem (ES) cells. The result shows significant neurotoxicity of both oligomers to the neurons, implying their relevance to the pathology of AD. Finally, the β and non-β oligomers are exposed to the OUI agitation. The result shows that the β oligomers are unaffected, while the non-β oligomers are transformed into fibrils. Thus, the β oligomers are independent dead-end products, not an intermediate aggregate in the fibrillation pathway.

MATERIALS AND METHODS

Preparation of Sample Solutions

Lyophilized-powder Aβ_{1-40} monomers were purchased from Peptide Institute (4307-v), which were dissolved by dimethyl-sulfoxide (DMSO) or ammonium water. (The ammonium water was used for samples for preparing the CD spectrum measurement, because DMSO generated a large absorbance background near 250 nm.) The final concentration of Aβ monomer was adjusted to 10 μM with 100 mM PBS (pH 7.4) containing 100 mM NaCl. The volume fractions to PBS of DMSO and ammonium in the final solutions are 20% and 0.05%, respectively. All prepared samples were frozen at -40 °C just before aggregation experiment. (Note that our sample solutions do not contain the ThT molecules.) All chemicals were purchased from Wako Pure Chemical Industries, Ltd.

Formation of β Oligomers by HSS Agitation

For introducing HSS agitation, a 500-μl sample solution was stirred by a polytetrafluoroethylene-coated stirring bar with different stirring speeds between 10 and 800 rpm at room temperature. The ThT level was measured every 30 min by picking a small amount of

sample solution and adding the ThT solution as described later.

Formation of Non-β Oligomers

It is reported that addition of excess NaCl ($\sim$500 mM) promotes the precipitation of oligomers without β-sheet structures.[22] We then added 500 mM NaCl for making the non-β oligomers: They were formed by incubating 50-μM Aβ_{1-40} monomer solution with 100 mM PBS containing 500 mM NaCl for 10 h at 37 °C, measuring the ThT level every 30-60 min. The formed oligomer solution was then diluted to 10 μM by 100 mM PBS without NaCl for the OUI agitation experiment.

OUI Agitation

Ultrasonic irradiation experiment was performed with the laboratory-built experimental system described in our previous paper.[24] Frequency and acoustic pressure of ultrasonic wave were controlled by changing the waveform for the ultrasonic transducer (TAMURA Corp., TBL4535D-28HB). We previously succeeded in accelerating the reaction for fibril nucleation of Aβ_{1-40} peptide with optimization of irradiation condition; the reaction rate constant for the fibril nucleation was increased by a factor of 850 with the ultrasonic wave with frequency of 29 kHz and the second-harmonics pressure of 80-90 kPa. We call the ultrasonic irradiation under these conditions the optimized ultrasonic irradiation (OUI). The temperature in the sample solution was set to 37 °C. OUI was applied to microtubes containing 500 μl sample solutions for 1 min, and the solutions were for 9 min. This 10 min sequence was repeated, and the ThT level was measured every 30-60 min. This OUI agitation yielded only fibrils; no amorphous-like aggregates were observed with transmission electron microscopy(TEM).

ThT Fluorescence Assay

The ThT powder (Wako Pure Chemical Industries, Ltd.) was diluted to final concentration of 5 μM by glycine-NaOH buffer (50 mM glycine, pH8.5). 50 μl of this 5-μM ThT solution and 5 μl sample solution was mixed in the quartz cell for the fluorescence measurement. The sample ThT level was measured by the spectrophotofluorometer, manufactured by JASCO Corporation (FP-6200), by taking the emission intensity at 485 nm with excitation at 450 nm. The ThT level was measured every 30-60 min.

Seeding Experiments

We prepared three kinds of seeds; (i)fibril-filament seeds. These were prepared by applying the OUI agitation to the standard monomer solution (10 μM Aβ_{1-40} in 100 mM PBS and100 mM NaCl) for 7 h. (ii) β-oligomer seeds, and (iii) non-β-oligomer seeds. The oligomer seeds were added to the standard monomer solution with volume fractions between 0.1% and 10%. The solution temperature was kept at 37 °C, and the ThT level was monitored.

CD Measurement

CD measurements were performed with the sample prepared with the ammonium water. We performed the measurement with the instrument by JASCO J-820. The light path length of quartz cell was 2 mm. The scanning range was 205 to 260 nm. We measured the spectra eight times for each sample and averaged them.

TEM Observations

The TEM observation was performed with H-7650 (HITACHI Corp.). Its acceleration voltage was set to 80 kV. First, the sample solution was put on a carbon-coated copper grid and incubated for 1 min. The sample solution was, then, stained by 2% ammonium molybdate solution.

QCM Measurement

We first prepared bare quartz chips with thicknesses of ∼28 μm (near 60 MHz resonance frequencies) by depositing 5-nm Cr thin film and then 25-nm Au thin film on both surfaces by magnetron sputtering method. Two chips with different resonance frequencies were rinsed with piranha solution for 5 min and cleaned by UV for 15 min.

The chips were immersed in a self-assembly-monolayer (SAM) solution (10 mM 10-carboxy-decanthiol (Dojindo, C385) in dehydrated ethanol) for 12 h at 4 °C. After activating the SAM terminals with the solution containing 100-mM 1-ethyl-3-(3- dimethylaminopropyl) carbodiimide (Dojindo, W001) and 100-mM N-hydroxysuccinimide (Wako, 087-09371) for 1 h, the target substances (β oligomer, non-β oligomer, or bovine serum albumin (BSA)) were immobilized on the SAM for 1 h. (The β oligomers were made by the 800-rpm HSS agitation for the 10-μM monomer standard solution for 5 h. Before immobilization, the β-oligomer solution was filtered with a 500-nm pore membrane. The non-β oligomers were prepared by incubation of 50-μM monomer solution with 500-mM NaCl for 4 h.) The activated binding sites without any substances were then blocked with BSA (10 mg/ml in PBS) for 1 h.

One of the quartz chip was immersed in 10 μg/ml OC antibody (StressMarq, SPC-507D) solution for 1 h and rinsed with PBS several times. We call this OC channel. The other quartz chip was immersed in 10 μg/ml A11 antibody (StressMarq, SPC-506D) solution for 1 h and rinsed with PBS several times. We call this A11 channel.

These chips were set on a handmade sensor cell, and their resonance frequencies were monitored simultaneously with a carrier buffer of 100-mM PBS containing 100-mM NaCl and 0.02% Tween 20 (National Diagnostics, EC-607) at a flow rate of ∼300 μl/min. After the resonance frequencies became stable, the staphylococcus-aureus protein A (SPA) solution with concentration of 50 μg/ml was injected.

Neutral Tissue Differentiation from Mouse Embryonic Stem Cells

The mouse BALB/c-derived ES cell line, ST1,[27] was differentiated to neural tissue by the modified SDIA method.[28] The differentiation medium was the 3:2 mixture of the fresh medium i.e. Glasgow's MEM (Thermo Fisher Scientific, Waltham, USA) containing 10% Knockout Serum Replacement (Thermo Fisher Scientific), 0.1 mM nonessential amino acids (Thermo Fisher Scientific), 1 mM sodium pyruvate (Thermo Fisher Scientific), 0.1 mM 2-mercaptoethanol (Sigma-Aldrich, St. Louis, USA) and its conditioned medium from the culture supernatant of MC3T3-G2/PA6 (PA6:RCB1127 from RIKEN Cell Bank, Ibaraki, Japan) for 24 hours. ST1 cells were cultured on the PA6 feeder layer which was prepared by ammonia treatment.[29] Medium change was once every 3 days and 3 weeks differentiation caused the neural tissue derived from ST1 cells. The ST1-derived neural tissues consisted by neurons, astrocytes, and oligodendrocytes.

Neurotoxicity Assay

After the neural tissue was derived from ST1 cells, 500 nM amyloid-β materials (monomers, β oligomers, and non-β oligomers) were added to the culture medium, and the cells were cultured for 1 or 3 days, and they were cultured for 6 or 4 days, respectively. We then evaluated the neurotoxicity by quantifying the amount of the remaining neurons with immunostaining shown below.

The tissues were fixed with 4% paraformaldehyde for 10 min and then permeabilized with 0.5% Triton X for 5 min. The fixed samples were incubated in Blocking One (Nacalai Tesque, Kyoto, Japan) for 30 min, then incubated with the primary antibody, Rabbit polyclonal Anti-betaGVTubulin antibody (1:1000; Abcam, Cambridge, UK), for 2 h and the secondary antibody, Alexa Fluor 594 Donkey anti-Rabbit IgG (1:200; Thermo Fisher Scientific), for 1 h. The samples were mounted in ProLong Gold Antifade Reagent (Thermo Fisher scientific) and observed using a fluorescence microscope. Each reagent was diluted with PBS. We washed the samples using PBS 3 times between all processes, and all reactions were carried

out at room temperature.

Obtained images were converted to 8-bit images and binarized by setting thresholds. The brightness of the image was inverted to count the non-stained region using the particle counting procedure. The stained region was then computed by subtracting the non-strained area from the total.

RESULTS

HSS Agitation Induces β Oligomer without Lag Time

Because we need to perform many aggregation experiments under stirring and ultrasonic agitations using identical peptide solution, we first prepared 30-ml 10-μM Aβ_{1-40} solution, divided it into many 500-μl samples, and froze them at -40 °C for storage before use. We checked the effect of the freezing step on the aggregation reaction under the HSS and OUI agitations with the ThT fluorescence assay. As shown in Figure 1a,b, there is no obvious difference between with and without freezing step, confirming that the frozen sample shows no specificity in aggregation reaction.

Figure 1c shows evolutions of the ThT fluorescence level of the Aβ_{1-40} solution caused by the stirring agitation with stirring speeds of 10, 100, and 800 rpm. The fluorescence level quickly increases without lag time and is saturated within a few hours. (The ThT level did not increase with other agitations such as the pipetting operation.) Thus, this aggregation reaction obeys the first-order reaction, and the concentration of the aggregate product $[P]$ will be explained by the exponential function,[30]

$$[P] = [M](1 - e^{-kt}). \tag{1}$$

Here, $[M]$ and k denote the initial monomer concentration and the reaction-velocity constant for the aggregation reaction, respectively. The reaction rate constant increases with increase

of the stirring speed (see inset in Figure 1c). Importantly, the reaction proceeds without lag time even with 10-rpm stirring agitation, being different from a typical amyloid-fibril formation, where the ThT level starts to increase after a long lag time.[31] The TEM observation reveals that the formed aggregates are spherical particles without any fibril-like structures as seen in Figure 1d. The particle diameter ranges between 20 and 30 nm, being similar to that reported in the previous works for the β oligomers.[13,14] Figure 1e shows the CD spectra measured for various sample solutions. The monomer solution exhibits the typical spectrum for the random coil state. The solution exposed to OUI shows the negative peak at 220 nm, corresponding to the well-developed β-sheet structure. (OUI actually caused only fibrils as will be shown.) The aggregates formed by the stirring agitations also show negative peaks near 225 nm, indicating that they possess β-sheet-like structures.[32] However, because the peak wavelength ($\sim$225 nm) is larger than that of fibrils, their β-sheet structures will be distorted. We consider the aggregates formed by HSS as the β oligomers, which will be confirmed with the seeding experiments and the QCM assay later. On the other hand, the oligomers formed under quiescent condition in the high NaCl-concentration (500 mM) solution show the typical spectrum of random coil structure (aqua line in Figure 1e). We here call this oligomer as the non-β oligomer.

Reactivity of β and Non-β Oligomers for OC and A11 Antibodies

Previous reports indicated that the β oligomers and non-β oligomers are recognized by OC and A11 antibodies, respectively.[11,13] We therefore performed immunoassay with these antibodies for our β and non-β oligomers by the two-channel WE-QCM biosensor system.[25,26] Schematic illustration of the assay is shown in Figure 2a. For investigating specificity between our β oligomer and the antibodies, we first immobilized the β oligomers on the two quartz crystal chips. After the blocking procedure with BSA, one of these was immersed in the OC-antibody solution (OC channel), and the other was in the A11 antibody solution (A11 channel). After the washing procedure, these two chips were set in the QCM cell, and

the SPA solution was injected. Because SPA specifically binds to the Fc domains of IgG molecules, it can be indicator for evaluating the specificity between the β oligomer and the reacted antibodies. Resonance frequencies of the two channels were simultaneously monitored, and the amount of the antibody captured by surface oligomers was evaluated through the frequency change caused by the SPA binding. Similar experiments were performed by immobilizing the non-β oligomer on the two sensor chips for investigating its specificity to OC and A11 antibodies. Examples of the reaction curves when the SPA solution was injected are shown in Figure 2b,c,d: The amount of the frequency change is significantly larger when the OC antibody was reacted to the β oligomers than when it was reacted to the A11 antibody or to BSA; Our β oligomer is recognized by the OC antibody. On the other hand, the frequency change becomes significantly larger when the A11 antibody was reacted to the non-β oligomer; the non-β oligomer is recognized by the A11 antibody. Figure 2e shows frequency changes at 30 min after arrival of the SPA solution for each experiment. Our β and non-β oligomers positively react to OC and A11 antibodies, respectively.

β and Non-β Oligomers cannot be Seeds for Fibrils

Because the reaction for fibril nucleation is the rate-limiting step on the fibril formation, addition of preformed fibril seeds to monomer solution accelerates the fibrillation, called the seeding reaction.[33,34] This allows evaluation for the regularity of β-sheet structure of the added materials. We then performed the seed experiments for investigating ordering of our β-sheet structure in the β oligomers induced by HSS, and non-β oligomers. The results are shown in Figure 3, which also includes the seed experiments for fibril seeds and non-β oligomers. In the spontaneous aggregation reaction without seeds, the ThT level remained unchanged for 10 h (blue circles). However, by adding seeds formed under the OUI agitation, the aggregation reaction immediately occurs without a lag time, being the typical seeding reaction. When the non-β oligomers are added as seeds (green plots), the ThT level remains

unchanged for all seed concentrations because of lack of the β-sheet structure. The β oligomer also cannot work as fibril seeds (red plots), indicating their distorted β-sheet structure.

Neurotoxicity Assay

Many studies related to the cytotoxicity of Aβ aggregates appear, where HeLa,[14] PC-12,[35,36] and neuroblastoma[37,38] cells were often adopted for evaluating the toxicity. On the other hand, some studies adopted primary murine neuronal cells,[39–41] being more suitable system to investigate their cytotoxicity, because they are closer to actual neurons. We here use the neuronal system differentiated from mouse ES cells, which include both of the neuron and glia cells (Figure 4a) for evaluating the neurotoxicity of the oligomers. Both of the oligomers were added to the culture medium to be a final concentration of 500 nM, and the cells were cultured for 1 day or 3 days. Then, the cells were cultured for a few days using the Aβ-free original medium. The neurons were stained and observed by the fluorescence microscopy. The representative fluorescence images are shown in Figure 4b,c,d,e, including results for negative control (only buffer solution) and monomer-added sample as control experiment. In the negative-control sample (Figure 4b), the axons intertangle with each other, forming the axon network; the axon density is high. In the case of monomer addition (Figure 4c), the axon density seems to be lower (its diameter seems to be smaller) than the negative control case. In the oligomer-addition cases (Figure 4d,e), the network structure is absent, and the axon density significantly decreases; the axons become thinner, shorter, and fragmented. Because the axons should become shorter and thinner when the cell body of neuron is damaged, we focus on the axon density as the degree of the neurotoxicity. The axon density is quantified by counting the immunostaining area. The result shows in the Figure 4f. Significant differences are found between the negative control and the oligomer-addition cases, confirming the neurotoxicity of our β and non-β oligomers.

Optimized Ultrasonic Irradiation to The Two Types Oligomers

The OUI agitation significantly increased the ThT level after ∼2.5 h lag time (red triangles), demonstrating its high ability to accelerate the aggregation reaction (Figure 5a). The aggregation reaction in this case thus includes nucleation and elongation phases, the typical fibril formation reaction of Aβ_{1-40} peptide. The aggregates formed at 6.5 h showed fibrils as shown in the TEM image in Figure 5a without any oligomeric aggregates.

We performed the OUI agitation followed by the HSS agitation for investigating the stability of the β oligomer. When the agitation was switched from OUI to HSS at 4.5 h (after saturation of the ThT level) (purple inverted triangles), no significant change was observed in the ThT level. Thus, the fibrils formed by the OUI agitation is unaffected by the HSS agitation because of high thermodynamic stability of fibrils. When the agitation was switched from HSS to OUI at 3 h (orange squares), where the ThT level was saturated, the ThT level did not increase and followed the behavior observed only with HSS (blue squares). The resultant morphology appears to be amorphous particles with ∼20 nm diameter as shown in the TEM image in Figure 5a. This is a surprising result, because OUI is a very powerful agitation to induce fibril formation; it can increase the reaction velocity constant for fibril nucleation by a factor of 850 compared with the nucleation reaction without OUI.[24] Thus, this result indicates that the β oligomers formed by the HSS agitation possess ultra-stable structures, which are unbreakable even with the OUI agitation.

On the other hand, the OUI agitation completely transforms the non-β oligomers into fibrils as shown in Figure 5b: The ThT level of the 50-μM Aβ_{1-40} solution with 500 mM NaCl remained unchanged for 16 h (open circles), and we confirmed amorphous aggregates at 10 h as shown in the TEM images in Figure 5b. However, when we applied OUI to the solution, the ThT fluorescence intensity increased, and fibril formation was observed as shown in the TEM images (solid circles). This result indicates that non-β oligomers are intermediates for fibrils as previously reported.[10,11]

DISCUSSION

Mechanical Denaturation Induced by HSS Forms the β Oligomers

The β oligomers are immediately formed by the HSS agitation (Figure 1c), and we attribute it to the shear stress caused by HSS, because β oligomers appear to be composed of twisted filaments about the internal helical axes;[14] the shear stress induces the torsional deformation on the aggregates, so that the formation of twisted structures will be enhanced. We estimate the shear stress in the solution under HSS with Taylor's equation,[42] assuming a homogenous isotropic turbulence flow. The dissipation rate in solution, ϵ, is defined by $\epsilon = \mu\langle\dot{\gamma}\rangle^2/2\rho$ with the solution viscosity ν, mass density ρ, and the average shear rate, $\langle\dot{\gamma}\rangle$. Taylor proposed that it is determined by the root-mean-square velocity U and a representative length in the system L as $\epsilon = C_\epsilon \cdot U^3/L$.[42] The dimensionless coefficient C_ϵ is known as Taylor's dissipation coefficient, and it converges to unity in higher speed flows.[42] We then set $C_\epsilon = 1$ and estimate the shear stress τ based on Newton's viscous law; $\tau = \mu \cdot \langle\dot{\gamma}\rangle$,

$$\tau \sim \sqrt{\frac{2\mu\rho U^3}{L}} \tag{2}$$

We used the inner diameter D=10 mm of the sample bottle for L and simply evaluate U with $U = D\omega/2$ with the angular velocity ω of the stirrer. Inset of Figure 1c shows the relationship between the shear stress and the stirring speed with the solid red line, displaying a correlation with the reaction rate constant for formation of the β oligomers. Jung and coworkers researched relationship between shear stress and strain of β-lactoglobulin monomer and reported that the shear strain γ reached $\sim$0.2 at the shear stress of $\tau = 0.8$ Pa,[43] implying that the shear modulus G ($=\tau/\gamma$) of the monomer becomes $\sim$4 Pa. The shear stress estimated under HSS reaches $\sim$4 Pa at 800 rpm, which could cause fairly large shear strain ($> \sim$1), when we assume the same shear modulus as the β-lactoglobulin monomer for Aβ_{1-40} monomer. Although the shear modulus is highly ambiguous, we expect that the HSS

causes a large shear strain to the monomer and aggregates.

Distortion of monomer is often required for proceeding to an aggregation reaction. For example, fibrillation of insulin is effectively carried out at elevated temperatures and lower pH.[44,45] These conditions are necessary for breaking the stable structure of the native monomer: Unfolded monomers by the high-temperature and low-pH condition polymerize to form thermodynamically more stable fibrils. Monomeric Aβ_{1-40} takes the β-strand structure in the fibrils.[46] Under the HSS agitation, the monomers exposed to the shear field interact with each other and may form the twisted fibril-like stacking. Thus, the deformation of monomers with the HSS agitation will induce formation of the β oligomer with distorted structure. The shear stress actually plays a principal role for structural transformation of proteins. For example, the in vivo role of shear flow in inducing the transition from globular native fold to the fibril state at a hydrophobic-hydrophilic interface has been reported.[47,48] It is important that the β oligomers thus shortly formed with the HSS agitation are significantly neurotoxic (Figure 4f). This knowledge will contribute to drug developments for AD.

β Oligomers are Independent Dead-End Products from Fibrils

We propose free energy landscape of aggregation reaction of Aβ_{1-40} peptide as shown in Figure 6a,b. We set the two oligomers at different states based on the results of CD measurement, the immunoassay with OC and A11 antibodies, and the OUI agitation experiment. We assume that aggregates will be produced before the the β-oligomer dead end; they correspond to intermediates in the pathway for the β oligomer. Because the β oligomer is easily formed by the HSS agitation, the energy barriers from monomer toward the β oligomer are lower than that for the fibril nucleation (Figure 6a): The shear stress is sufficient for producing the pathway from monomers to the β oligomer through the β-oligomer intermediates, but it is insufficient to surpass the high energy barrier for nucleation; fibril is, therefore, hardly formed with HSS.

On the other hand, OUI drastically decreases the energy barrier for nucleation by the cavitation effects[24] as explained in Figure 6c: The direct conversion from monomers into nuclei is made possible as follows: The ultrasonic cavitation bubble repeats the bubble nucleation, expansion, and collapse, responding to the ultrasonic period. The bubble collapse significantly increases the solution temperature near the bubble. The monomers are attached on the cavitation-bubble surface via their hydrophobic residues, they move with bubble surface, they are highly densified at the bubble collapse, and they are transiently heated at the collapse, resulting in producing the nuclei.[24] This mechanism will apply to the non-β oligomers, because their diameter ($\sim$ 10 nm) is much smaller than the bubble diameter ($\sim$ 10 μm) (Figure 6c). Actually, the non-β oligomers are immediately transformed into fibrils as seen in Figure 5b. In addition, the inherent ultrasonic decomposition effect unravels weakly interacting aggregates and decompose them into monomers (Figure 6d), including the non-β oligomers and the intermediates for the β oligomers. (OUI apparently increases energy levels of the intermediates.) The decomposed monomers can be directly transformed into the fibrils via the cavitation effect above. Therefore, all unstable intermediates, including the non-β oligomers, are eventually transformed into fibrils, and this view consistently explains our observations that we cannot find any oligomer species under the OUI agitation and that we cannot generate the β oligomers with OUI.

Surprisingly, once the β oligomers are formed, they were unaffected even by the OUI agitation, which is the powerful and pathway-oriented agitation for fibrillation. This indicates high thermodynamic stability of the β oligomer state, and we conclude that the β oligomer should be an independent dead-end product of the different pathway from that for fibrils.

It is highly important to recognize that such a neurotoxic and ultrastable Aβ oligomer is easily and shortly produced under HSS. These achievements will contribute not only to scientific understanding of the Aβ aggregation reaction, but also to understanding the pathogenic mechanism for AD.

CONCLUSIONS

In this study, we formed two types of oligomers, β and non-β oligomers, and confirmed their physical-chemical characteristics using ThT fluorescence assay, CD spectrum measurement, immunoassay with fibril-specific and oligomer-specific antibodies, and seeding reaction. The HSS agitation can form the β oligomers in a few hours by their shear-stress field, potentially being useful as a method to form the β oligomers in a short time. Furthermore, their neurotoxicity to the nerve system differentiated from the mouse ES cells was confirmed. We used the optimized-ultrasonic-irradiation agitation to discuss the stability of the two types oligomers and find that the β oligomers are ultrastable. Thus, the optimized ultrasonic irradiation becomes an effective method to evaluate the stability of protein aggregates.

AUTHOR INFORMATION

Corresponding Authors

*E-mail ogi@me.es.osaka-u.ac.jp (H.O.).

Author Contributions

K.N. performed ultrasonic-irradiation and stirring experiments and wrote this paper. M.S. performed TEM observation and CD experiments. K.T. and Y.T. performed the neurotoxicity assay. M.H. contributed to construction of the ultrasonic-irradiation system. Y.G. contributed to modeling the results. H.O. produced this study and wrote paper.

ABBREVIATIONS

Aβ, amyloid β; AD, Alzheimer disease; ThT, thioflavin-T; TEM, transmission electron microscopy; CD, circular dichroism; OUI, optimized ultrasonic irradiation; HSS, high speed

stirring; ES cell; embryonic stem cell

Acknowledgement

This study was supported by the Funding Program for Next Generation World-Leading Researchers (Next Program) by the Cabinet Office, Government of Japan.

References

(1) Norlin, N.; Hellberg, M.; Filippov, A.; Sousa, A. A.; Grobner, G.; Leapman, R. D.; Almqvist, N.; Antzutkin, O. N. Aggregation and Fibril Morphology of the Arctic Mutation of Alzheimer's Aβ Peptide by CD, TEM, STEM and in Situ AFM. *J. Struct. Biol.* **2012**, *180*, 174-189.

(2) Tsigelny, I. F.; Sharikov, Y.; Kouznetsova, V. L.; Greenberg, J. P.; Wrasidlo, W.; Gonzalez, T.; Desplats, P.; Michael, S. E.; Trejo-Morales, M.; Overk, C. R.; et al. Structual Diversity of Alzheimer's Disease Aβ Dimers and Their Role in Oligomerization and Fibril Formation. *J. Alzheimers Dis.* **2014**, *39*, 583-600.

(3) Tipping, K. W.; van Oosten-Hawle, P.; Hewitt, E. W.; Radford, S. E. Amyloid Fibres: Inert End-Stage Aggregates or Key Players in Disease? *Trends Biochem. Sci.* **2015**, *40*, 719-727.

(4) Prusiner, S. B. Prions. *Proc. Natl. Acad. Sci. USA* **1998**, *95*, 13363-13383.

(5) Spillantini, M. G.; Schmidt, M. L.; Lee, V. M.; Trojanowski, J. Q.; Jakes, R.; Goedert, M. Alpha-synuclein in Lewy bodies. *Nature* **1997**, *388*, 839-840.

(6) Balducci, C.; Beeg, M.; Stravalaci, M.; Bastone, A.; Sclip, A.; Biasini, E.; Tapella, L.; Colombo, L.; Manzoni, C.; Borsello, T.; et al. Synthetic amyloid-β oligomers impair

long-term memory independently of cellular prion protein. *Proc. Natl. Acad. Sci. USA* **2010**, *107*, 2295-2300.

(7) Ladiwala, A. R.; Litt, J.; Kane, R. S.; Aucoin, D. S.; Smith, S. O.; Ranjan, S.; Davis, J.; Van Nostrand, W. E.; Tessier, P. M. Conformational Differences between Two Amyloid β Oligomers of Similar Size and Dissimilar Toxicity. *J. Biol. Chem.* **2012**, 287, 24765-24773.

(8) Ohnishi, T.; Yanazawa, M.; Sasahara, T.; Kitamura, Y.; Hiroaki, H.; Fukazawa, Y.; Kii, I.; Nishiyama, T.; Kakita, A.; Takeda, H.; et al. Na, K-ATPase α3 is a Death Target of Alzheimer Patient Amyloid-β Assembly. *Proc. Natl. Acad. Sci. USA* **2015**, *112*, 4465-4474.

(9) Barucker, C.; Bittner, H. J.; Chang, P. K.-Y.; Cameron, S.; Hancock, M. A.; Liebsch, F.; Hossain, S.; Harmeier, A.; Shaw, H.; Charron, F. M.; et al. Aβ_{42}-oligomer Interacting Peptide (AIP) Neutralizes Toxic Amyloid-β_{42} Species and Protects Synaptic Structure and Function. *Sci. Rep.* **2015**, *5*, 15410.

(10) Kayed, R.; Head, E.; Thompson, J. L.; McIntire, T. M.; Milton, S. C.; Cotman, C. W.; Glabe, C. G. Common Structure of Soluble Amyloid Oligomers Implies Common Mechanism of Pathogenesis. *Science* **2003**, *300*, 486-489.

(11) Kayed, R.; Head, E.; Sarsoza, F.; Saing, T.; Cotman, C. W.; Necula, M.; Margol, L.; Wu, J.; Breydo, L.; Thompson, J. L.; Rasool, S.; et al. Fibril Specific, Conformation Dependent Antibodies Recognize a Generic Epitope Common to Amyloid Fibrils and Fibrillar Oligomers That is Absent in Prefibrillar Oligomers. *Mol. Neurodegeneration* **2007**, *2*, 18.

(12) Chang, E. S.-H.; Liao, T.-Y.; Lim, T.-S.; Fann, W.; Chen, R. P.-Y. A New Amyloid-Like β-Aggregate with Amyloid Characteristics, Except Fibril Morphology. *J. Mol. Biol.* **2009**, *385*, 1257-1265.

(13) Wu, J. W.; Breydo, L.; Isas, J. M.; Lee, J.; Kuznetsov, Y. G.; Langen, R.; Glabe, C. G. Fibrillar Oligomers Nucleate the Oligomerization of Monomeric Amyloid but Do Not Seed Fibril Formation. *J. Biol. Chem.* **2010**, *285*, 6071-6079.

(14) Stroud, J. C.; Liu, C.; Teng, P. K.; Eisenberg, D. Toxic Fibrillar Oligomers of Amyloid-β Have Cross-β Structure. *Proc. Natl. Acad. Sci. USA* **2012**, *109*, 7717-7722.

(15) Kato, M.; Kinoshita, H.; Enokita, M.; Hori, Y.; Hashimoto, T.; Iwatsubo, T.; Toyo'oka, T. Analytical Method for β-Amyloid Fibrils Using CE-Laser Induced Fluorescence and Its Application to Screening for Inhibitors of β-Amyloid Protein Aggregation. *Anal. Chem.* **2007**, *79*, 4887-4891.

(16) Necula, M.; Kayed, R.; Milton, S.; Glabe, C. G. Small Molecule Inhibitors of Aggregation Indicate That Amyloid β Oligomerization and Fibrillization Pathways Are Independent and Distinct. *J. Mol. Biol.* **2007**, *282*, 10311-10324.

(17) Adachi, M.; So, M.; Sakurai, K.; Kardos, J.; Goto, Y. Supersaturation-limited and Unlimited Phase Transitions Compete to Produce the Pathway Complexity in Amyloid Fibrillation. *J. Biol. Chem.* **2015**, *290*, 18134-18145.

(18) Levin, A.; Mason, T. O.; Adler-Abramovich, L.; Buell, A. K.; Meisl, G.; Galvagnion, C.; Bram, Y.; Stratford, S. A.; Dobson, C. M.; Knowles, T. P. J.; et al. Ostwald's Rule of Stages Governs Structural Transitions and Morphology of Dipeptide Supramolecular Polymers. *Nat. Commun.* **2014**, *5*, 5219.

(19) Miti, T.; Mulaj, M.; Schmit, J. D.; Muschol, M. Stable, Metastable, and Kinetically Trapped Amyloid Aggregate Phases. *Biomacromol.* **2014**, *16*, 326-335.

(20) Chatani, E.; Lee, Y.-H.; Yagi, H.; Yoshimura, Y.; Naiki, H.; Goto, Y. Ultrasonication-Dependent Production and Breakdown Lead to Minimum-Sized Amyloid Fibrils. *Proc. Natl. Acad. Sci. USA* **2009**, *106*, 11119-11124.

(21) So, M.; Yagi, H.; Sakurai, K.; Ogi, H.; Naiki, H.; Goto, Y. Ultrasonication-Dependent Acceleration of Amyloid Fibril Formation. *J. Mol. Biol.* **2011**, *412*, 568-577.

(22) Yoshimura, Y.; Lin, Y.; Yagi, H.; Lee, Y. H.; Kitayama, H.; Sakurai, K.; So, M.; Ogi, H.; Naiki, H.; Goto, Y. Distinguishing Crystal-Like Amyloid Fibrils and Glass-Like Amorphous Aggregates from Their Kinetics of Formation. *Proc. Natl. Acad. Sci. USA* **2012**, *109*, 14446-14451.

(23) Nakajima, K.; Nishioka, D.; Hirao, M.; So, M.; Goto, Y.; Ogi, H. Drastic Acceleration of Fibrillation of Insulin by Transient Cavitation Bubble. *Ultrason. Sonochem.* **2017**, *36*, 206-211.

(24) Nakajima, K.; Ogi, H.; Adachi, K.; Noi, K.; Hirao, M.; Yagi, H.; Goto, Y. Nucleus Factory on Cavitation Bubble for Amyloid β Fibril. *Sci. Rep.* **2016**, *6*, 22015.

(25) Ogi, H.; Motohisa, K.; Matsumoto, T.; Hatanaka, K; Hirao, M. Isolated Electrodeless High-Frequency Quartz Crystal Microbalance for Immunosensors. *Anal. Chem.* **2006**, *78*, 6903-6909.

(26) Ogi, H.; Nagai, H.; Fukunishi, Y.; Yanagida, T.; Hirao, M.; Nishiyama, M. Multichannel Wireless-Electrodeless Quartz-Crystal-Microbalance Immunosensor. *Anal. Chem.* **2010**, *82*, 3957-3962.

(27) Aikawa, H.; Tamai, M.; Mitamura, K.; Itmainati, F.; Barber, G. N.; Tagawa, Y. Innate Immunity in an In Vitro Murine Blastocyst Model Using Embryonic and Trophoblast Stem Cells. *J Biosci Bioeng.* **2014**, *117*, 358-365.

(28) Kawasaki, H.; Mizuseki, K.; Nishikawa, S.; Kaneko, S.; Kuwana, Y.; Nakanishi, S.; Nishikawa, S.; Sasai, Y. Induction of Midbrain Dopaminergic Neurons from ES Cells by Stromal Cell-Derived Inducing Activity. *Neuron* **2000**, *28*, 31-40.

(29) Abraham, S.; Riggs, M. J.; Nelson, K.; Lee, V.; Rao, R. R. Characterization of human fibroblast-derived extracellular matrix components for human pluripotent stem cell propagation. *Acta Biomater.* **2010**, *6*, 4622-33.

(30) Chiti, F.; Taddei, N.; Baroni, F.; Capanni, C.; Stefani, M.; Ramponi, G.; Dobson, C. M. Kinetic Partitioning of Protein Folding and Aggregation. *Nat. Struct. Biol.* **2002**, *9*, 137-143.

(31) Watzky, M. A.; Morris, A. M.; Ross, E. D.; Finke, R. G. Fitting Yeast and Mammalian Prion Aggregation Kinetic Data with the Finke-Watzky Two-Step Model of Nucleation and Autocatalytic Growth. *Biochemistry* **2008**, *47*, 10790-10800.

(32) Woody, R. W. Circular Dichroism. *Methods Enzymol.* **1995**, *246*, 34-71.

(33) Jarrett, J. T.; Lansbury Jr., P. T. Seeding "One-Dimensional Crystallization" of Amyloid: A Pathogenic Mechanism in Alzheimer's Disease and Scrapie? *Cell* **1993**, *73*, 1055-1058.

(34) Ohhashi, Y.; Kihara, M.; Naiki, H.; Goto, Y. Ultrasonication-induced Amyloid Fibril Formation of β_2-Microglobulin. *J. Mol. Biol.* **2005**, *280*, 32843-32848.

(35) Vaisid, T.; Barnoy, S.; Kosower, N. S. Calpastatin Overexpression Attenuates Amyloid-β-Peptide Toxicity in Differentiated PC12 Cells. *Neurosci.* **2008**, *156*, 921-931.

(36) Diaz, J. C.; Simakova, O.; Jacobson, K. A.; Arispe, N.; Pollard, H. B. Small Molecule Blockers of the Alzheimer Aβ Calcium Channel Potently Protect Neurons from Aβ Cytotoxicity. *Proc. Natl. Acad. Sci. USA* **2009** *106*, 3348-3353.

(37) Picone, P.; Carrotta, R.; Montana, G.; Nobile, M. R.; Biagio, P. L. S.; Carlo, M. D. Aβ Oligomers and Fibrillar Aggregates Induce Different Apoptotic Pathways in LAN5 Neuroblastoma Cell Cultures. *Biophys. J.* **2009**, *96*, 4200-4211.

(38) Zameer, A.; Kasturirangan, S.; Emadi, S.; Nimmagadda, S. V.; Sierks, M. R. Anti-Oligomeric Aβ Single-Chain Variable Domain Antibody Blocks Aβ-Induced Toxicity Against Human Neuroblastoma Cells. *J. Mol. Biol.* **2008**, *384*, 917-928.

(39) Ahmed, M.; Davis, J.; Aucoin, D.; Sato, T.; Ahuja, S.; Aimoto, S.; Elliott, J. I.; Nostrand, W. E. V.; Smith, O. S. Structural Conversion of Neurotoxic Amyloid-β (1-42) Oligomers to Fibrils. *Nat. Struct. & Mol. Biol.* **2010**, *17*, 561-567.

(40) Romito-DiGiacomo, R. R.; Menegay, H.; Cicero, S. A.; Herrup, K. Effects of Alzheimer's Disease on Different Cortical Layers: The Role of Intrinsic Differences in Aβ Susceptibility. *J. Neurosci.* **2007**, *27*, 8496-8504.

(41) Cheng, J. S.; Dubal, D. B.; Kim, D. H.; Legleiter, J.; Cheng, I. H.; Yu, G. Q.; Tesseur, I.; Wyss-Coray, T.; Bonaldo, P.; Mucke, L. Collagen VI Protects Neurons against Aβ Toxicity. *Nat. Neurosci.* **2008**, *12*, 119-121.

(42) McComb, W. D.; Berera, A.; Salewski, M.; Yoffe, S. Taylor's (1935) Dissipation Surrogate Reinterpreted. *Phys. Fluids* **2010**, *22*, 061704.

(43) Jung, J.-M.; Gunes, D. Z.; Mezzenga, R. Interfacial Activity and Interfacial Shear Rheology of Native β-Lactiglobulin Monomers and Their Heat-Induced Fibers. *Langmuir* **2010**, *26*, 15366-15375.

(44) Malisauskas, M.; Weise, C.; Yanamandra, K.; Wolf-Watz, M.; Morozova-Roche, L. Lability Landscape and Protease Resistance of Human Insulin Amyloid: A New Insight into Its Molecular Properties. *J. Mol. Biol.* **2010**, *396*, 60-74.

(45) Muta, H.; Lee, Y.-H.; Kardos, J.; Lin, Y.; Yagi, H.; Goto, Y. Supersaturation-Limited Amyloid Fibrillation of Insulin Revealed by Ultrasonication. *J. Biol. Chem.* **2014**, *289*,18228-18238.

(46) Petkova, A.; Ishii, Y.; Ballbach, J. J.; Antzutkin, O. N.; Leapman, R. D.; Delaglio, F.; Tycko, R. A Structural Model for Alzheimer's β-Amyloid Fibrils Based on Experimental Constraints from Solid State NMR. *Proc. Natl. Acad. Sci. USA* **2002**, *99*, 16742-16747.

(47) Mangione, P. P.; Esposito, G.; Relini, A.; Raimondi, S.; Porcari, R.; Giorgetti, S.; Corazza, A.; Fogolari, F.; Penco, A.; Goto, Y.; et al. Structure, Folding Dynamics, and Amyloidogenesis of D76N β_2-Microglobulin: Roles of Shear Flow, Hydrophobic Surfaces, and α-Crystallin. *J. Biol. Chem.* **2013**, *288*, 30917-30930.

(48) Stoppini, M.; Bellotti, V. Systemic Amyloidosis: Lessons from β_2-Microglobulin. *J. Biol. Chem.* **2015**, *290*, 9951-9958.

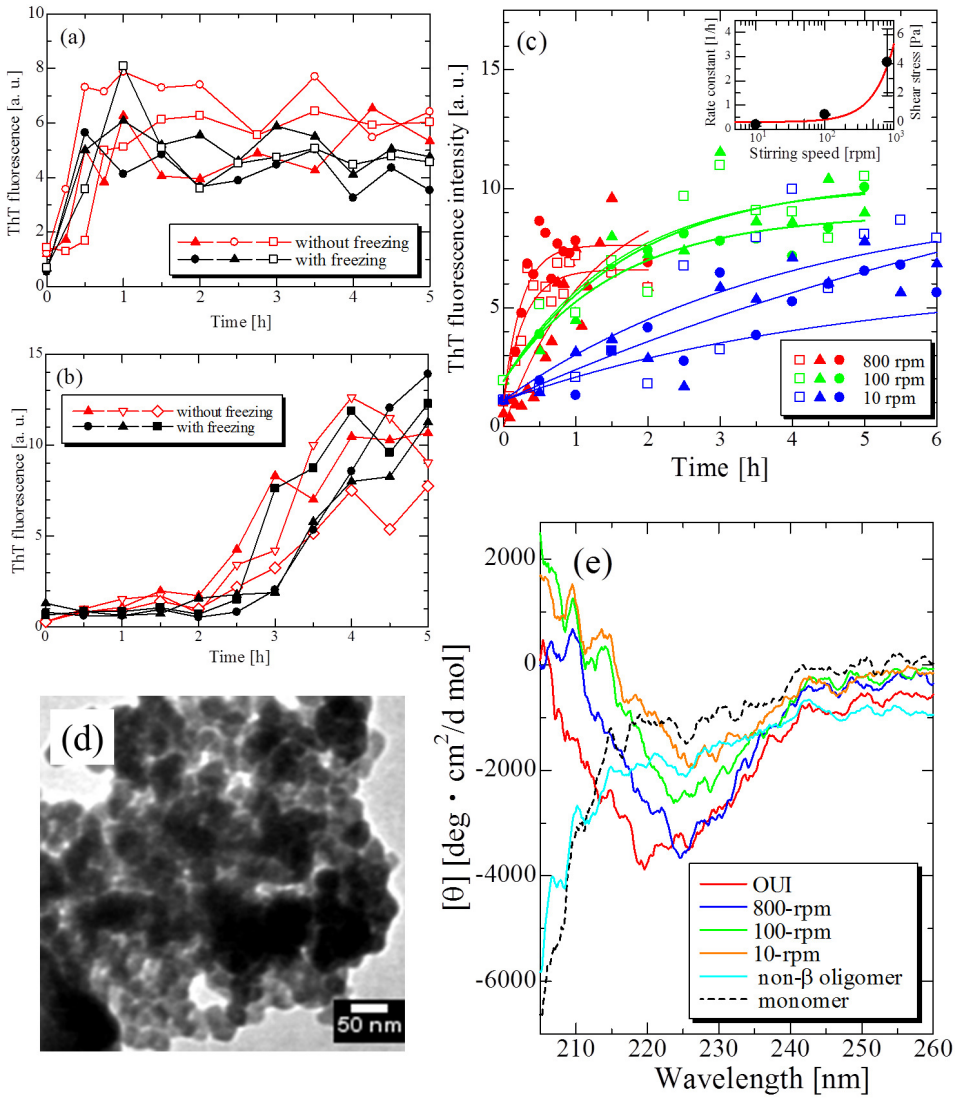

Figure 1: Time evolutions of ThT fluorescence intensity of samples with and without the freezing step under (a)HSS at 800 rpm and (b)OUI(29 kHz) agitations (showing three independent measurements). (c) Time evolutions of the fluorescence intensity under various stirring speeds, 10, 100, and 800 rpm. (Three independent measurements are shown.) Inset shows relationship between stirring speed, rate constant for formation of the β oligomers, and estimated shear stress. (d) TEM image of the β oligomer formed by 800-rpm HSS agitation. (e) CD spectra of Aβ aggregates formed under various conditions.

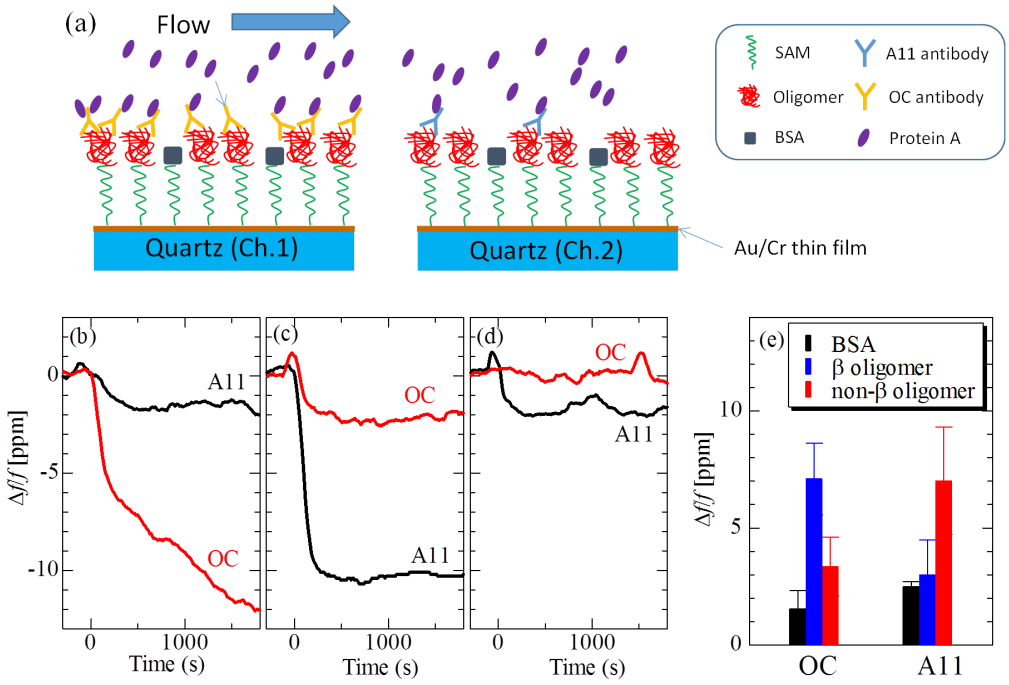

Figure 2: (a) Schematic illustration of an immunoassay with WE-QCM measurement system for investigating the reactivity of the oligomers to OC and A11 antibodies. Frequency changes for three sensor chips, on which (b) the β oligomers, (c) the non-β oligomers, and (d) BSA were immobilized and then exposed to OC and A11 antibodies. The horizontal axis indicates the time measured from the injection of the staphylococcus-aureus protein A (SPA) solution. The vertical axis indicates the fractional frequency change. (e) The amounts of frequency changes in the QCM assay for the β and non-β oligomers and BSA chips. The error bars denote the standard deviation among three independent measurements.

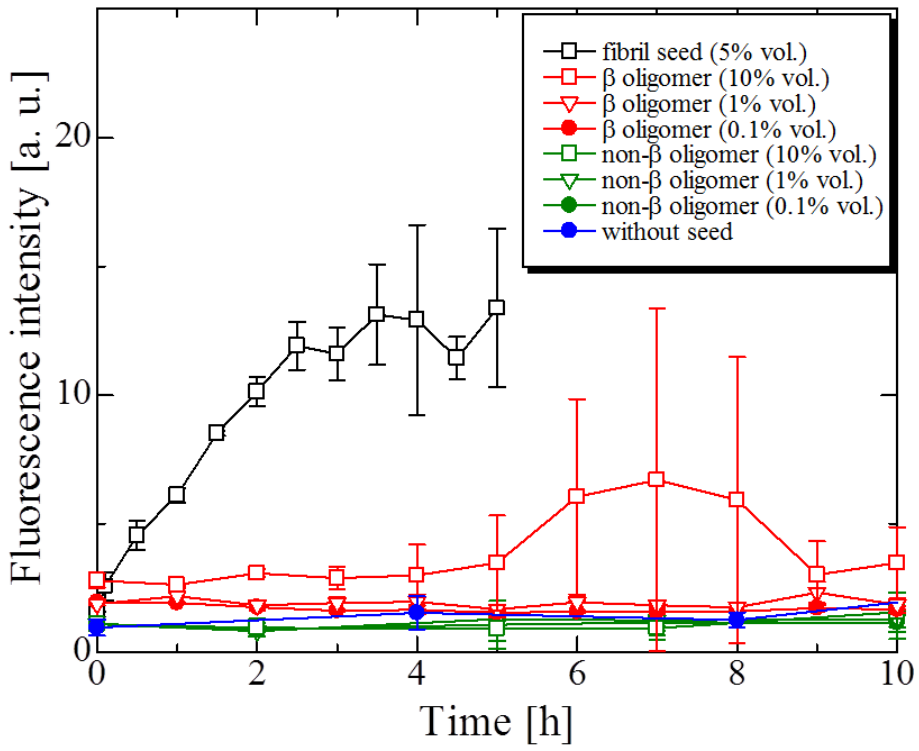

Figure 3: Changes of the ThT fluorescence intensity in the seed experiments at 37 °C. The OUI fibril seeds fabricated by the OUI agitation (black squares) quickly cause fibrillation without lag time, whereas the β oligomers (red marks) fail to work as the seeds for fibrils. The non-β oligomers also fail to become the fibril seeds. Three independent seeding experiments were performed for each seed, and their average values are plotted with the standard-deviation error bars.

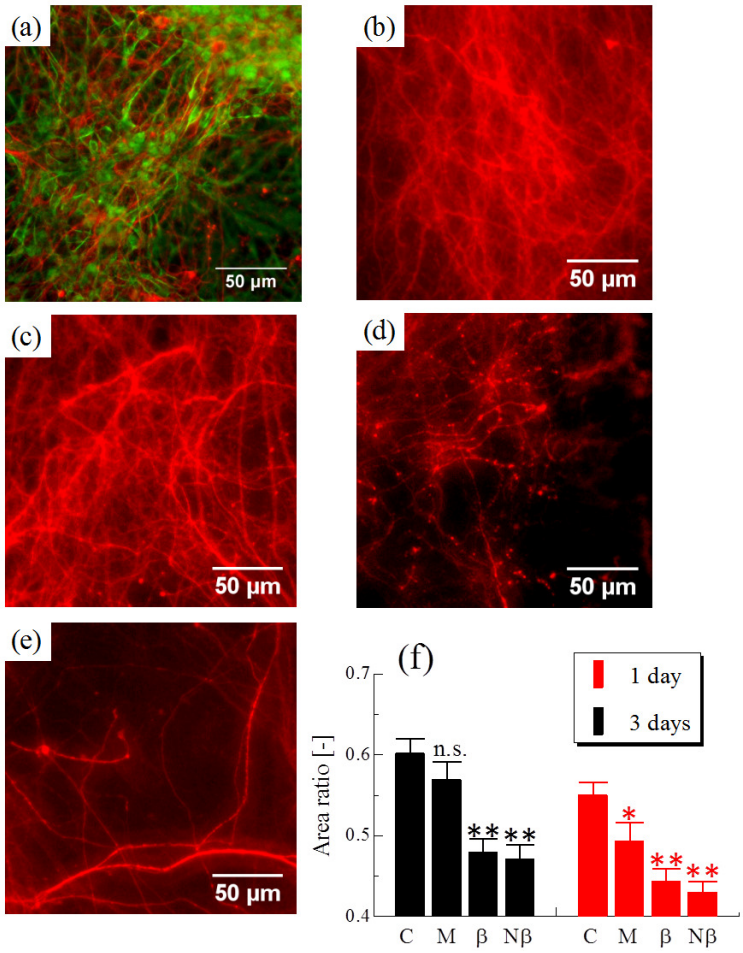

Figure 4: (a) Fluorescence image of the neural system differentiated from mouse ES cells. Red and green regions indicate neuron and astrocyte structures, respectively. (b)-(e) are fluorescence images of axons after the neurotoxicity assay; (b) negative control, (c) monomer-, (d) β-oligomer-, and (e) non-β-oligomer added samples. (f) Comparison of the axon density calculated among above four samples. C, M, β, and Nβ denote control, monomer, β oligomer, and non-β oligomer, respectively. Results represent the mean$\pm$sem (n=15-25). n.s.: not significant, *p $<$ 0.05, and **p $<$ 0.001 versus leftmost bars in the each group, negative control.

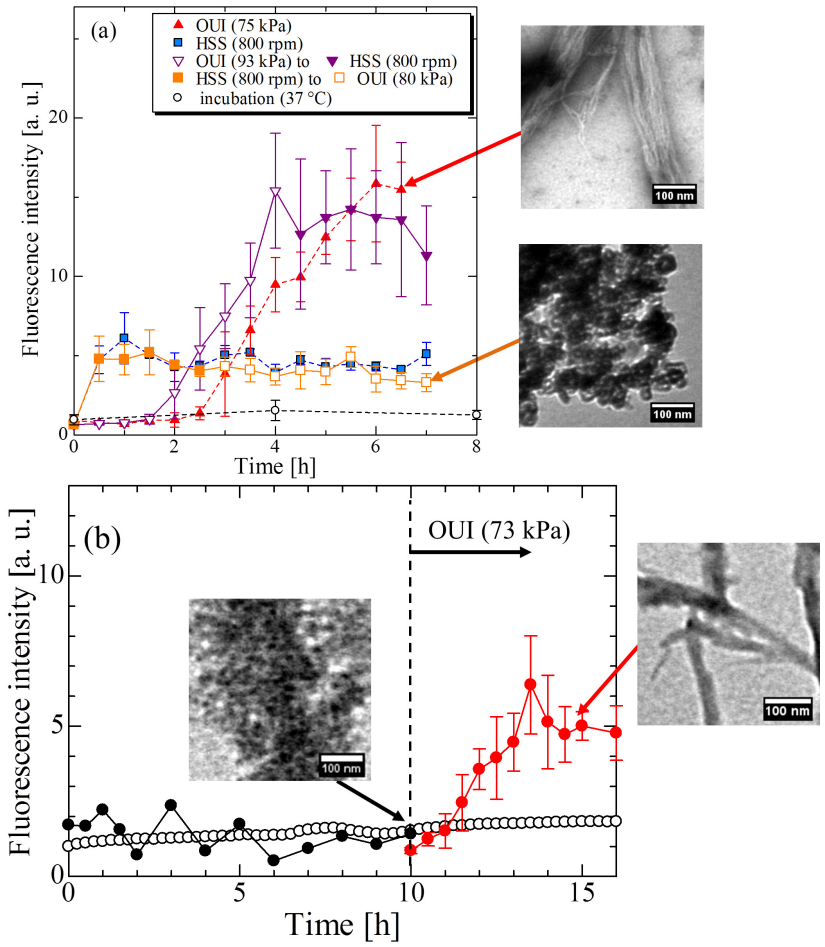

Figure 5: (a) Time courses of the ThT fluorescence intensity caused by HSS agitation, OUI agitation, HSS-to-OUI agitation, OUI-to-HSS agitation, and incubation. Error bars denote the standard deviation among three independent experiments. The pressure value in the OUI agitation denotes the second harmonics pressure of irradiated ultrasonic wave, which expresses the net ultrasonic energy spent in the solution.[24] TEM images show amyloid fibrils formed by the OUI agitation and the β oligomers exposed to the HSS-to-OUI agitation, respectively. (b) Time evolution of the ThT level during formation of the non-β oligomers (open circles) and that during the OUI agitation to the non-β oligomers (red solid circles). Insets show TEM images of the non-β oligomers and aggregates formed by applying the OUI agitation to the non-β oligomers, clearly showing that OUI transforms the non-β oligomers into fibrils.

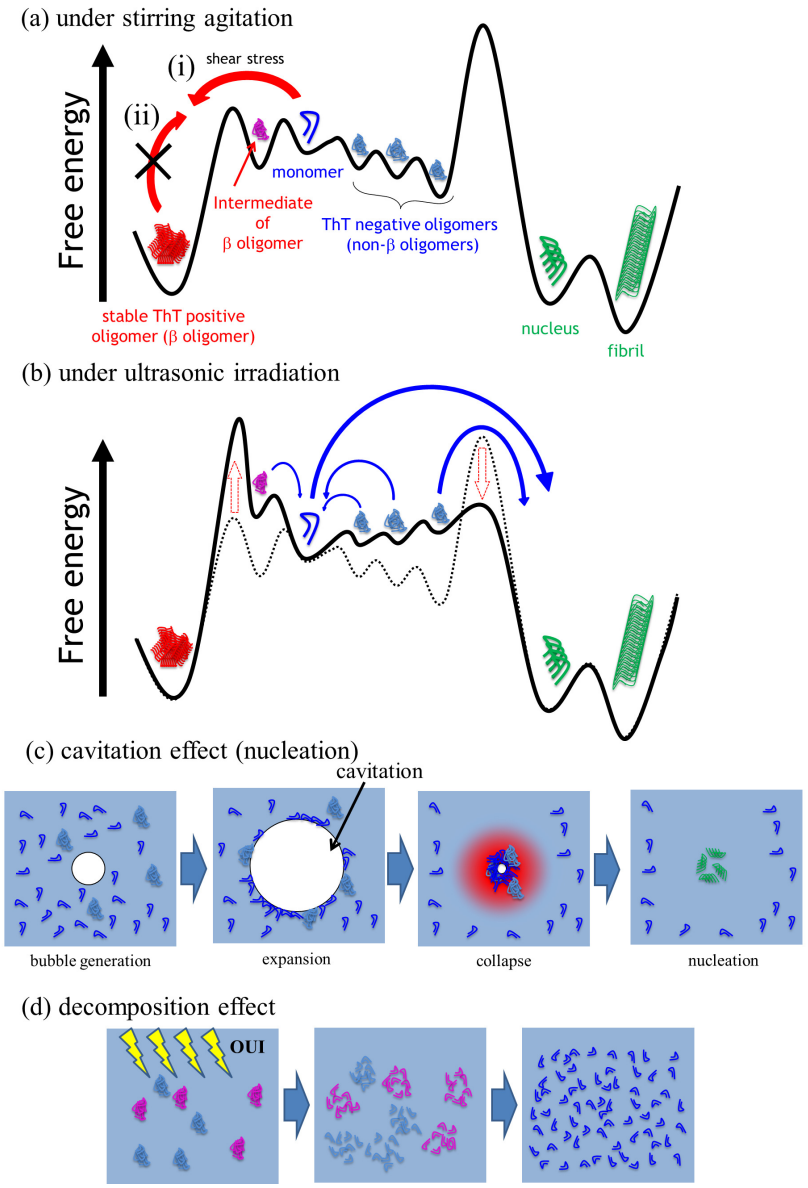

Figure 6: Proposed free-energy landscapes of Aβ_{1-40} aggregation reaction under (a) HSS and (b) OUI. (a) (i) ThT-positive oligomers (β oligomers) are formed with shear stress generated by the HSS agitation . (ii) Once the β oligomers are formed, their conformations are unchanged even under the OUI agitation, despite that OUI is a very powerful agitation tool to induce fibrillation. (b) OUI accelerates nucleation of fibril by apparently lowering the energy barrier for nucleation through the cavitation effect (c).[24] The non-β oligomers are changed their conformation into fibrils directly by the cavitation effect (c) or through their disassociation to monomers by the ultrasonic decomposition effect (d) and then by the cavitation effect (c). The intermediate aggregates on the β oligomer pathway are also eventually transformed into fibrils through their decomposition to monomers, so that the β oligomer cannot be formed under OUI. Therefore, energy states of any unstable intermediates are apparently heightened under OUI.

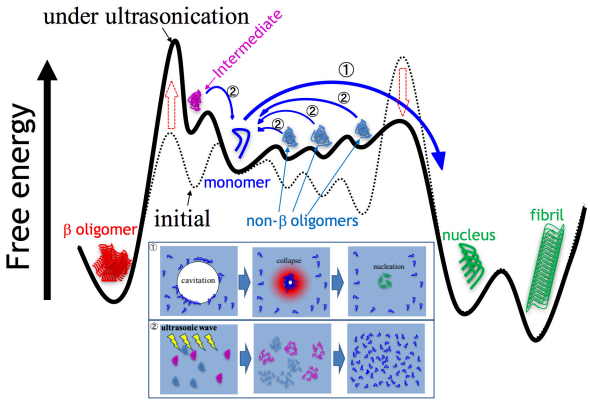
under ultrasonication
Intermediate
Free energy
β oligomer
initial
monomer
non-β oligomers
nucleus
fibril
①
②
cavitation
collapse
nucleation
ultrasonic wave

TOC graphic